*seeds*

MDPI

*Article*

# Mutation in the *LONGIFOLIA1* Gene Resulted in Suppressed Insensitivity of *Arabidopsis thaliana proteolysis6* Mutant to Ethylene During Seed Germination

**Xu Wang [1], Ying Luo [1], Yuan Cao [1], Yujin Gong [1], Francoise Corbineau [2] and Yong Xiang [1,*]**

[1] Shenzhen Branch, Guangdong Laboratory of Lingnan Modern Agriculture, Genome Analysis Laboratory of the Ministry of Agriculture and Rural Affairs, Agricultural Genomics Institute at Shenzhen, Chinese Academy of Agricultural Sciences, Shenzhen 518120, China; wangxu03@caas.cn (X.W.); luoying980306@outlook.com (Y.L.); caoyuan32@outlook.com (Y.C.)

[2] Biologie des Semences, UMR 7622, IBPS, Sorbonne Université, 4 Place Jussieu, 75005 Paris, France; francoise.corbineau@sorbonne-universite.fr

* Correspondence: xiangyong@caas.cn

## Abstract

Seed dormancy and germination is regulated by internal hormones and exogenous environment cues. Ethylene is one of the hormones that break seed dormancy and induce seed germination. Our previous study showed that N-degron pathway gene, *proteolysis6* (*PRT6*) was involved in dormancy release by ethylene, the defection of which exhibiting ethylene-insensitivity in *Arabidopsis thaliana*. In the present study, through screening an ethyl methyl sulfonate-mutagenized (EMS) population of *prt6−1*, we isolated a recessive mutant that acted as a suppressor of *prt6* that rescued its insensitivity to ethylene as well as a phenotype of shorter silique length. Further bulk segregant analysis on F2 population identified a premature termination located in the third exon of *LONGIFOLIA1* (*LNG1*), previously reported in the regulation of longitudinal cell elongation. Mutation of *LNG1* in *prt6−1* background by CRISPR-Cas9 confirmed that *LNG1* was epistatic to *PRT6* in seed responsiveness to ethylene. Our finding proposed the pleiotropic effect of *LNG1* in seed dormancy breakage by ethylene via *PRT6*, providing novel functional component at the downstream of the coordinated *PRT6* and ethylene signaling pathway.

**Keywords:** *PRT6*; ethylene; BSA-seq; *LNG1*; silique length

check for updates

Academic Editor: Aria Dolatabadian

Received: 3 August 2025
Revised: 5 September 2025
Accepted: 24 September 2025
Published: 30 September 2025

**Citation:** Wang, X.; Luo, Y.; Cao, Y.; Gong, Y.; Corbineau, F.; Xiang, Y. Mutation in the *LONGIFOLIA1* Gene Resulted in Suppressed Insensitivity of *Arabidopsis thaliana proteolysis6* Mutant to Ethylene During Seed Germination. *Seeds* **2025**, *4*, 48. https://doi.org/10.3390/seeds4040048

**Copyright:** © 2025 by the authors. Licensee MDPI, Basel, Switzerland. This article is an open access article distributed under the terms and conditions of the Creative Commons Attribution (CC BY) license (https://creativecommons.org/licenses/by/4.0/).

## 1. Introduction

Primary seed dormancy refers to the inability of seeds to germinate in apparently favorable conditions at harvest, while secondary dormancy is considered as a quiescent state of the seed induced by unfavorable conditions [1,2]. The transition from dormancy to germination is critical for the generative reproduction in the plant life cycle. The induction and breakage of seed dormancy depends on genetic and environmental factors [1,2]. Ethylene, a gaseous hormone, has been reported to release seed dormancy of many species via fine-tuning of the dominant hormone balance of abscisic acid (ABA)/gibberellins (GAs) and reactive oxygen species (ROS) [3–6]. Moreover, ethylene promotes the endosperm cap weakening and possibly enhances water transport after seed imbibition [7,8]. In several species, germination completion is concomitant with the endogenous ethylene production [6,9,10].

Classical ethylene signaling is identified from the "triple response". It starts from ethylene perception and binding by receptors, which inactivates and inhibits the function

of CTR1 (CONSTITUTIVE TRIPLE RESPONSE 1), thus allowing EIN2 (ETHYLENE INSENSITIVE 2) to act as a positive regulator of ethylene and facilitating the accumulation of EIN3. EIN3 as the central transcription factor binds to the promoters of some *ERF* (*ETHYLENE RESPONSIVE FACTORS*) to regulate transcription of downstream genes [6,11,12]. The effect of ethylene in seed dormancy control was proven by the significant dormancy level alterations in ethylene receptor mutants [13–16]. It was proposed that increased seed dormancy was present in the gain-of-function mutant, like *ethylene response1−2* (*etr1−2*), while the reduced seed dormancy in loss-of-function mutant, such as *etr1−6*, *etr1−7* or *reduced dormancy3* (*rdo3*) [16]. It was recently elucidated that ERF12 functioned downstream of the ethylene receptor ETR1 and formed a repressive complex with TOPLESS (TPL) that inhibited the expression of *DELAY OF GERMINATION1* (*DOG1*), a conserved central regulator of seed dormancy [16]. Dormancy release by ethylene required the production of reactive oxygen species (ROS), a prerequisite for radicle elongation during the germination process, in which mitochondria was suggested to be the major intracellular source [17].

The N-degron pathway corresponds to the ubiquitin-proteasome system (UPS) degradation by targeting specific N-terminal residue of a protein [18]. In Arabidopsis, two N-recognins, namely, PROTEOLYSIS 1 (PRT1) and PRT6 acted as E3 ligase identifying specific N-degrons, the aromatic residues (Phe, Trp, Tyr) and the basic residues (Arg, His, Lys), respectively. These N-degrons could be generated by proteolytic cleavage such as N-terminal Met excision by methionine aminopeptidase (MAP) or endoproteolytic cleavage by endopeptidase (EP). In addition, N-degrons is also able to be produced through successive process, firstly, post-translational modification of tertiary residues (Asn, Gln, Cys) to secondary residues (Asp, Glu, Cys-sulfinic acid) via deamidation or oxidation; finally, a peptide initiating with Arg via Arginyl-tRNA transferase (ATE) is subjected to identification by PRT6 [18,19]. The N-degron pathway has been reported to regulate many aspects of plant development and adaptation to the environment. In recent years, particular attention has been paid to the involvement of PRT6 in oxygen sensing with the identification of the first substrate, Ethylene Response Factor transcription factors VII (ERFVIIs), including RELATED TO APETALA (RAP) 2.12, RAP2.2, and RAP2.3, HYPOXIA-RESPONSIVE ERF (HRE) 1 and HRE2 [20,21]. The second and third substrates of PRT6, LITTLE ZIPPER 2 (ZPR2) and VERNALIZATION 2 (VRN2) were proposed in the regulation of plant development, also in an oxygen dependent manner [22–24]. All the substrates mentioned above begin with Met-Cys and functioned as N-degrons in their pre-pro-protein forms, a feature that has facilitated their discovery despite the diversity and complexity of neo-N-termini. The effect of *PRT6* in the regulation of seed germination was first reported in regard to the involvement of ABA signaling with the enhanced sensitivity of *prt6* to ABA, compromised sensitivity of *prt6aba insensitive3* (*abi3*) or *prt6abi5* to ABA in seed germination [25]. Further studies showed that *PRT6* promoted seed germination by destabilizing ERFVIIs through nitric oxide, a key molecule in dormancy release. ERFVIIs, in turn, directly bind to the *ABI5* promoter and enhance its expression, thereby mediating the crosstalk between nitric-oxide and ABA signaling during seed germination [26]. Our previous study showed that *prt6* mutant were ethylene-insensitive during seed germination. And their canonical substrates, the ERFVIIs transcription factors RAP2.2, RAP2.3, and RAP2.12, functioned downstream of PRT6 in the ethylene response with the enhanced sensitivity to ethylene in *prt6rap2.2rap2.3rap2.12* [27,28].

In order to discover a novel component of *PRT6*−involved pathway in the control of seed responsiveness to ethylene other than the well-known substrates, we launched out a genetic screening for the *prt6−1* suppressors from an ethyl methane sulfonate (EMS) mutant library. A recessive mutant, *prt6−r*, was subsequently isolated that exhibited increased seed sensitivity to ethylene and produced shorter siliques. Our study not only de-

scribed the identification of the suppressor but also provided insights for future molecular-mechanism investigations.

## 2. Materials and Methods

### 2.1. Plant Materials and Growth Condition

T-DNA insertion mutant *prt6−1* (SAIL−1278−H11) in *Arabidopsis thaliana* Columbia background was obtained from the Nottingham Arabidopsis Stock Center (NASC). For seed multiplication, *prt6−r* (isolated from the EMS mutant library of *prt6−1*), the F1 and F2 hybrid populations of *prt6−1* and *prt6−r* seeds were firstly cold stratified at 4 °C for 3 days to break dormancy then transferred into the potting mixture (2:1 mixture of Pindstrup substrate and vermiculite) placed in a growth chamber under a 16 h light/8 h dark cycle (23 °C/20 °C). Siliques were harvested at maturity and seeds were stored at −20 °C before experiment.

### 2.2. EMS Mutagenesis

Arabidopsis *prt6−1* seeds were imbibed in 0.1% KCl (MedChemExpress, Shanghai, China) at 4 °C for 16–20 h, rinsed with tap water, and treated with 0.1 mM EMS (Biorigin, Beijing, China) at room temperature for 6–8 h. After discarding the EMS solution, seeds were neutralized in 0.1 M sodium thiosulfate (Macklin, Shanghai, China) for 30 min, rinsed in running tap water for 12 h, suspended in 0.3% agar (Forscience, Beijing, China), and immediately sown onto the potting mixture.

### 2.3. Screening of Suppressors of prt6−1 Mutant

EMS-mutagenized *prt6−1* seeds (M0) were grown and the seeds were harvested altogether as M1 without evaluating any parameters. M2 seeds were harvested from the mother plant of each M1 individual. Newly harvested M2 seeds were used to perform a seed germination test with/without the treatment of ethylene (See Section 2.7). The M2 seeds with enhanced sensitivity (>80% germination percentage) to ethylene in germination were kept for further propagation. Around 30 individuals for each family of M2 population were grown and each individual was harvested as M3. A seed germination test with/without the treatment of ethylene (See Section 2.7) was also carried out on the M3 population. The stable mutant individuals were confirmed by the stability of the phenotype of significant sensitivity to ethylene in germination (>80% germination percentage) carried out continuously in M4 and M5.

### 2.4. Population Construction and Bulk DNA Preparation

Seeds of *prt6−1* and the *prt6−r* mutant were planted and hybridized to generate F1, one single of F1 were grown to develop a F2 population. A total of 523 F2 individuals and the two parental lines were planted. Siliques from each individual were harvested at maturity and seeds were stored at −20 °C to keep dormancy for ethylene treatment. Genomic DNA was isolated from fresh young leaves of each F2 plant using the procedure of the CTAB method [29]. The grinded leaves were added with CTAB buffer (Macklin, Shanghai, China) and incubated at 65 °C to break down the cells. The supernatant was collected and mixed with chloroform–isoamyl alcohol to separate DNA. The upper aqueous phase was added with isopropanol to precipitate DNA and the final pellets were washed by ethanol. Two genomic DNA bulks were established for the F2 population with extremely contrasting differences in the phenotypes of seed germination and silique length. Each bulk consisted of around 20 individuals with equal DNA concentration, which were evaluated by Qubit 4 TM Fluorometer (Thermo Fisher Scientific, Wilmington, NC, USA) with dsDNA

HS Assay Kit (Vazyme, EQ121, Nanjing, China) as the manufacturer's user guide. The DNA bulks were then used for whole-genome sequencing.

### 2.5. BSA-Seq Analysis

The DNA bulks and DNA samples from parents were sent to the MGI DNBSEQ-T10 platform for library construction and sequencing. Raw reads were firstly cleaned by fastp [30]. The subsequent cleaned reads were mapped to the Tair10 genome using bwa [31]. The mapping files were processed into BAM files using the SAMtools software version 1.6 [32]. Meanwhile, the duplicates were removed by picard version 2.18.29 (https://broadinstitute.github.io/picard/, accessed on 1 August 2025). The software gatk version 4.2.3 was used for variant calling and filtering across all samples simultaneously using standard hard filtering parameters [33]. The generated VCF files were then used to calculate the SNP index via the sliding window method. The delta (SNP index) was obtained by subtracting SNP-index (1) from that of SNP-index (2), which was integrated into the QTLseq pipline [34]. G prime statistic algorithm method analysis was carried out with the utilization of QTLseqr [35]. SNP annotation was performed based on the Tair10 genome using the annovar software version 2020.06.08 [36].

### 2.6. CRISPR-Cas9 Editing

*LNG1* genome-edited lines were generated using the egg cell specific promoter derived CRISPR/Cas9 vector, pHK2-AtCas9-U6 (BioRun, Wuhan, China), which contained a ccdB cassette flanked by two BsaI sites. The forward and reversed oligos (Sangon, Guangzhou, China) were synthesized with BsaI overhangs and 20 bp spacer (Primer sequences shown in Supplementary Data). The single-stranded primers were firstly annealed, and the products were digested and ligated together with pHK2-AtCas9-U6 vector by BsaI enzyme (NEB) and T4 DNA ligase (NEB). The positive construction was selected by transformation into E.coli DH5$\alpha$ and confirmed by colony sequencing. For plant genetic transformation, the fused vector was transformed into *Arabidopsis thaliana prt6−1* with *Agrobacterium tumefasciens* strain GV3101 by floral dip method [37]. The T0 generations were sprayed with glufosinate ammonium (Yeason, Shanghai, China) in early seedling stages to select positive transformation. In the T1 and T2 generations, the homozygous lines were identified by genome PCR and sequencing near the spacer site.

### 2.7. Germination Assays with Ethylene Treatment

Germination assays were carried out in a 2.6 L tightly closed container injected with or without gaseous ethylene (5%) (HDX, Shenzhen, China). The seed responsiveness to ethylene test was conducted with 100 μL/L concentration. For the germination test, seeds were placed on three layers of filter paper moistened with deionized water at 25 °C. Seeds were considered to have germinated as soon as the radicle protruded through the seed coat. Germination percentages were calculated after 7 days. Results corresponded to the mean of the germination percentages obtained with at least three biological replicates of 50–100 seeds from independent mother plants.

### 2.8. Silique Length Measurement

In order to count the average silique length of each individual from F2 population, we adopt a more convenient statistical method. After the silique maturation, the first six developed siliques from the main inflorescence axis were taken and the average silique length was then calculated.

## 3. Results

### *3.1. Phenotypic Characterization of prt6−r and Bulk Construction*

The *prt6−r* mutant was identified from EMS-based mutagenesis in the genetic background of T-DNA mutant *prt6−1*, which was reported the insensitivity to ethylene in seed germination from our previous research [27]. The mutant *prt6−r* not only repressed the insensitivity to ethylene, but also exhibited shorter siliques (Figure 1A,B).

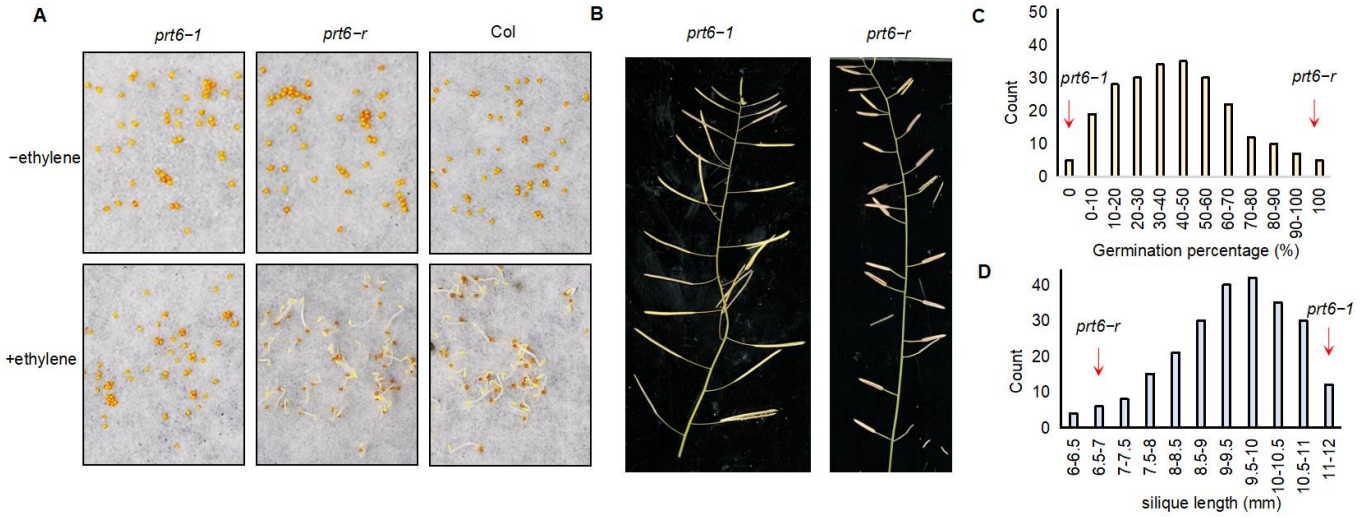


**Figure 1.** Analysis of the phenotypes of *prt6−1*, *prt6−r*, and the F2 population. (**A**) Germination of *prt6−1* and *prt6−r* in the presence or absence of ethylene at 25 °C in the dark; (**B**) siliques of *prt6* and *prt6−r*; (**C**) distribution of seed germination percentage in the presence of ethylene from 237 F2 accessions; (**D**) distribution of silique length from 243 F2 accessions.

For rapid identification of the gene controlling the two phenotypes, especially seed sensitivity to ethylene, we crossed the *prt6−r* mutant to original line, *prt6−1* to obtain F1 progeny. F1 plants were self-pollinated to generate F2 progeny for bulk construction. Silique lengths from each individual of the F2 population were firstly measured as described in Section 2 The silique length distribution in a total of 243 accessions exhibited a positively skewed distribution pattern (Figure 1D). Subsequently, freshly harvested seeds from 243 individuals were firstly subjected to the test of the dormant level, that is, germination assay at 25 °C in the dark without ethylene. Only non-germinated accessions were kept for further ethylene treatment. This procedure excluded 6 lines with relatively lower dormancy. The germination percentage distribution in the presence of ethylene in a total of 237 accessions was shown a negatively skewed distribution (Figure 1C). Both of the distribution patterns indicated that the germination and silique length of *prt6−r* might be a recessive trait. Based on the phenotype of the progenies, the first 15% and the last 15% in the population of "germination percentage" and "silique length" were taken into consideration for bulk construction. Two bulks were developed for sequencing, bulk1 habor 33 progenies with germination percentage with ethylene < 20% and average silique length > 10 mm, and bulk2 habor 17 progenies with germination percentage with ethylene > 80% with ethylene and their silique length were less than 7.5mm. Therefore, the preliminary dormancy test without ethylene treatment and the recruitment of the evaluation on two quantitative traits improved the accuracy of BSA (Bulked-segregant analysis)-seq.

### *3.2. Quality Control of Whole-Genome Sequencing Data*

Genomic DNA from bulk1, bulk2, and the two parents were subjected to whole-genome sequencing using MGI-DNBSEQ-T10 platform (BGI, Shenzhen, China). The generated raw data was firstly removed from the adaptor sequence. Meanwhile, low-quality

reads that had a mass value of Q ≤ 5 and accounted for more than 50% of the entire read were also removed. Thus, quality control of the sequencing data was conducted to retain only the qualified data before performing any further analyses. Following the trimming and filtering, clean data were obtained with an average Q30 of 88.50% (Table 1), signifying that the bases were sequenced precisely and hence retained a high quality that allows for the identification of candidate genomic variations between the two bulks. The sequence data were compared with the reference genome of Tair10 to determine the genome coverage and mapping rate. The bulk1 covered a mapping rate of 99.69% for the whole genome with 99.16% mapping rate, while the bulk2 covered 99.68% for the whole genome with 99.42% mapping rate. These values indicated high-quality mapping results and the better homogeneity of the sequencing data with the reference sequence (Table 1).

**Table 1.** Quality of the sequencing data and mapping data for the bulked samples and parents.

| | Clean Base/G | Q30/% | GC Content/% | Mapped Reads | Mapped Rate/% | Coverage/% | Average Depth |
|---|---|---|---|---|---|---|---|
| bulk1 | 23.84 | 87.87 | 37 | 154,147,804 | 99.16 | 99.69 | 137 |
| bulk2 | 19.75 | 86.45 | 36 | 125,074,857 | 99.42 | 99.68 | 113 |
| *prt6* | 24.41 | 87.23 | 36 | 151,180,273 | 99.75 | 99.68 | 152 |
| *prt6−r* | 30.71 | 92.46 | 41 | 124,972,640 | 63.44 | 99.69 | 126 |

### *3.3. Genomic Variation Distribution and Annotation*

The software gatk was used for SNPs and insertion/deletion (InDel) calling for the two pools and parents following the alignment of the reads to Tair10 genome. The further annovar algorithm was used to perform annotation and classification of all the variations that were identified. The variation in SNP occurs when a single nucleotide of A, T, C, or G differs between samples or individuals, while InDels are the insertions and deletions of small DNA fragments. In total, 21,185 variants were detected with 15,745 (74.32%) SNPs and 5440 (25.68%) InDels, respectively (Supplementary Dataset S1) (Figure 2). The distribution of the variants tended to be located at the downstream, upstream, and intergenic regions, whereas the variants located at the exon or splicing site only accounted for 4.16%, among which a total of 2125 variants resulted in missense or silent mutation (Supplementary Dataset S1). In addition, the identified base pair substitution patterns indicated that the most common nucleotide change was C:G > T:A, which was consistent with the previous report of the preference of EMS-induced mutation [38].

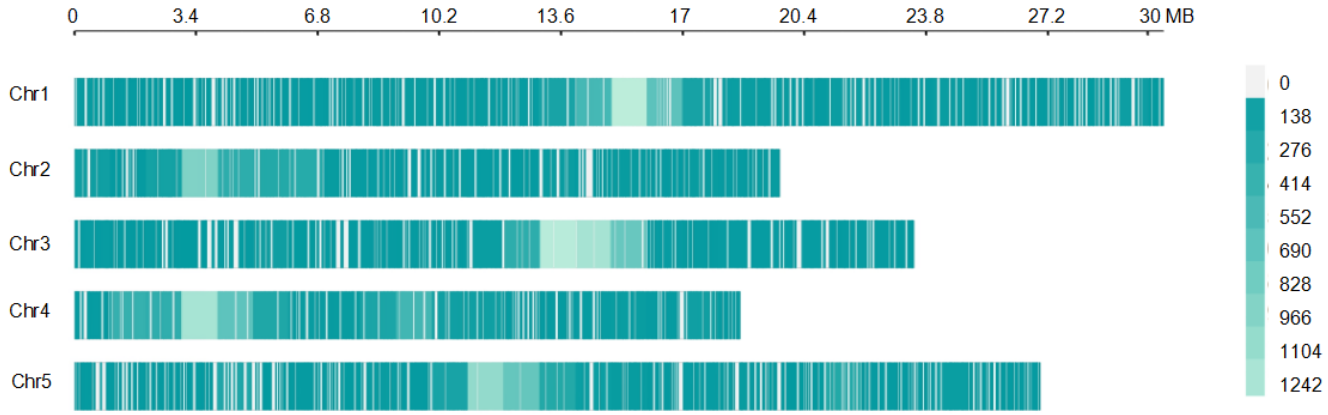


**Figure 2.** Variant distributions across two bulks and parents on the chromosomes of *Arabidopsis thaliana*. The marker density is indicated by different bar colors.

### *3.4. BSAseq Based on G′ Value Method and Delta SNP Method*

The G′ value is a modified statistic obtained after smoothing the G statistic which was proposed in the BSA studies [39]. We mapped putative genomic regions with a q-value at the false discovery rate of 0.05 for the approach of G′ value. The distribution of the G′ value across five chromosomes revealed that four genomic regions, 17.3–18.2 Mb on chromosome 1, 14.0–14.6 Mb on chromosome 3, 4.8–5.6 Mb, and 12.4–13.2 Mb on chromosome 5, were highly linked to seed sensitivity to ethylene and silique length (Figure 3) (Supplementary Dataset S2). In addition, among them, one peak on chromosome 5, spanning from 4.8 to 5.6 Mb, exhibited the highest mean G′ value, indicating that it was major QTL with the application of the G′ statistic (Figure 3). Based on the approach of sliding window of the whole genome, we calculated SNP index, followed by plotting the △SNP index for all five chromosomes according to the QTLseq pipeline [34] (Figure 4). The SNP index represents frequencies of parental alleles in the population of bulked individuals. In this case, the Tair10 genome was used as the reference, where an SNP-index of 1 indicates that reads in the population are derived from the EMS mutant allele *prt6−r* genome, whereas SNP-index = 0 indicates the reads are derived only from original *prt6* genome. It was shown that the SNP index of bulk2 from one region of chromosome 5 was close to 1, while the SNP index of bulk1 from this region was much lower than the remaining regions, which resulted in a significant candidate region at 4.1–7.8 Mb on chromosome 5 with the △SNP index above 99% confidence interval (Figure 4, Supplementary Figure S1). The finding here coincided with one of the regions using the G′ statistic method (Figures 3 and 4). Likewise, a third method, Mutmap was also recruited, which used the sequence of the original cultivar to polarize the site frequencies of neighboring markers with an unexpected site frequency. It confirmed again that the region (4.3–5.5 Mb) on chromosome 5 harbored the gene responsible for the mutant phenotype (Supplementary Figure S2).

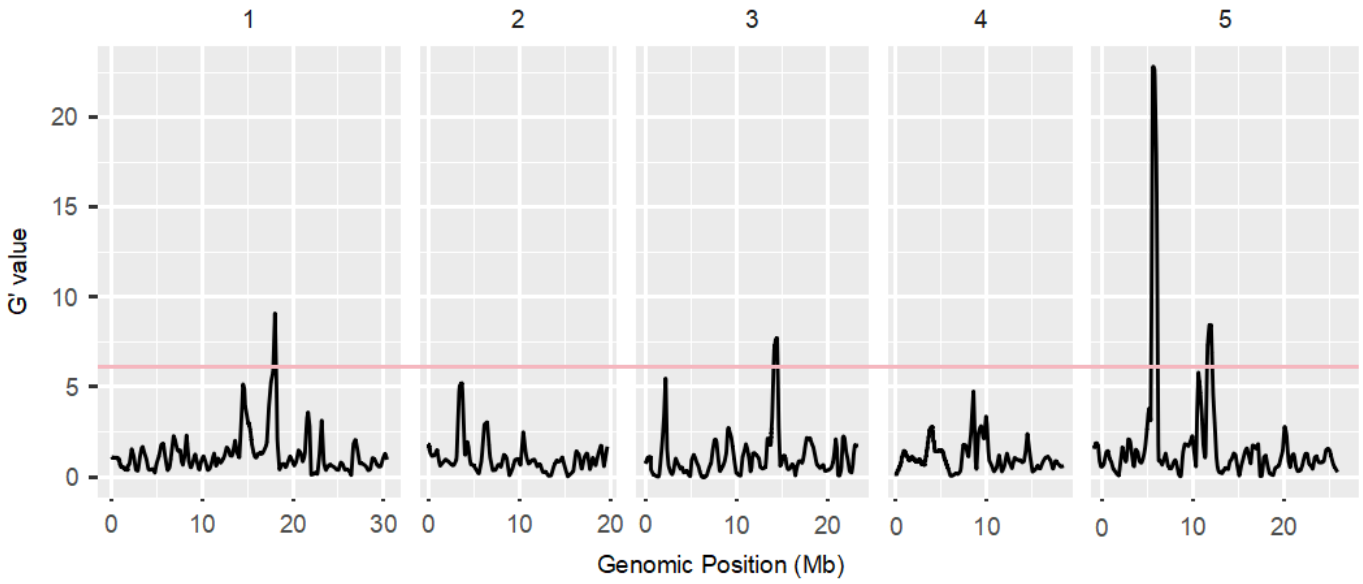


**Figure 3.** Chromosomal distributions of smoothed G′ value for SNP and InDel. Plots produced by the plotQTLStats function from QTLseqr with 1 Mb sliding window. The genome-wide false discovery rate threshold of 0.05 is indicated by the red line.

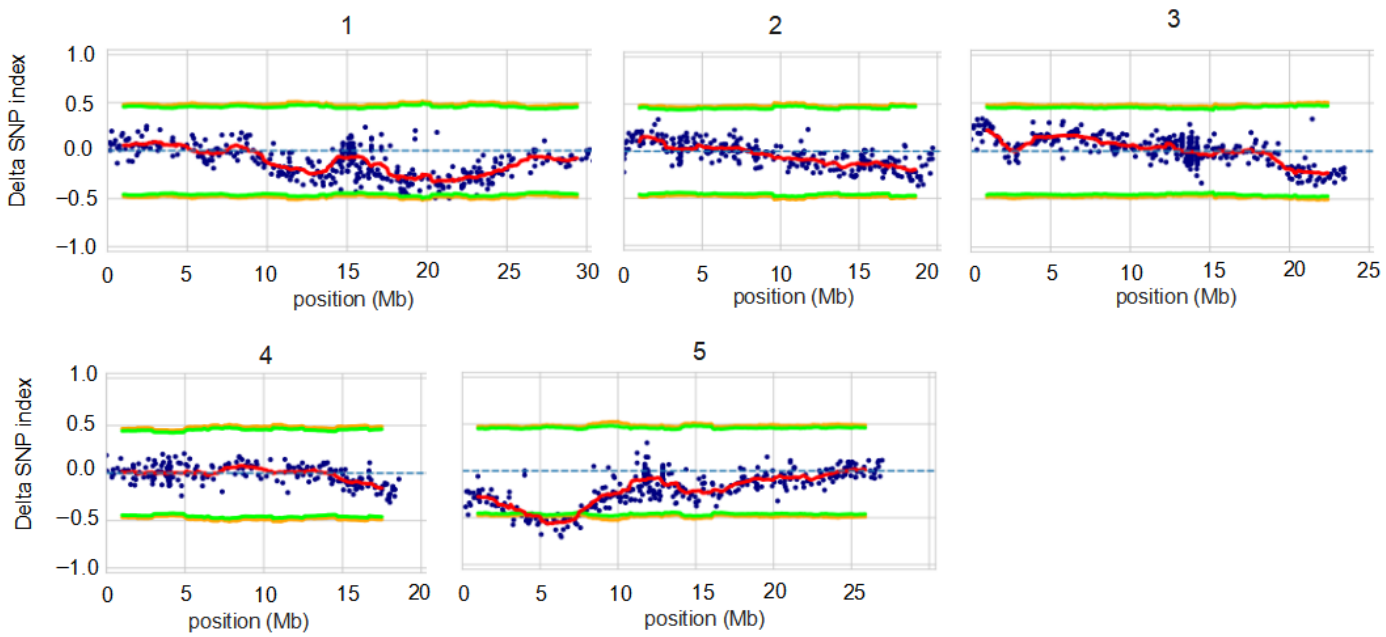


**Figure 4.** The distribution of ΔSNP-index values across all the five chromosomes. The ΔSNP-index values were calculated using a sliding window of 2 Mb physical intervals with a 100 kb step size. The blue dots represented the variants; the red line represented mean SNP-index; the orange line and the green line represented mean 99% ($p < 0.01$) and mean 95% ($p < 0.05$) confidence interval, respectively.

### *3.5. Annotation of Candidate Variants and Candidate Gene Confirmation*

Subsequent variants annotation at 4.1–7.8 Mb on the chromosome 3 were classified according to gene distance and location such as downstream, upstream, exonic, intronic, and intergenic, and the variants located in the exonic region were further annotated into stopgain, splicing stie, nonsynonymous, synonymous and so on. After filtering, a total of 12 variants in this region had resulted in higher effect by impact, such as non-synonymous or stopgain (Table 2). Based on the gene description of the 12 genes, only one gene *AT1G15580* (*LNG1*), was speculated as a potential candidate considering the reported function in the regulation of cell expansion of several organs [40]. A point C to T mutation in *LNG1* on the third exon led to a premature stop (Figure 5A). Moreover, we noticed that the SNP index from bulk2 on the candidate region was close to 1, indicating that most of the sequencing reads generated from the bulk2 harbored the variations; while the SNP index from bulk1 was not near 0, with an average value of 0.43, suggesting that the selection of the extreme individuals in this bulk was slightly biased. Even so, the case above was not that bizarre considering that it was often tricky to phenotype quantitative traits and the phenotypes we investigated in our study, seed dormancy and seed silique length, were prone to being affected by the environment.

In order to verify our speculation, we constructed the knock-out of *LNG1* in *prt6−1* background by CRISPR-cas9-mediated gene editing technology, generating two alleles with 1 bp insertion and 2 bp deletion in the 3rd exon of *LNG1* (Figure 5D) (Supplementary Figures S3 and S4). Further germination assay and silique length measurement confirmed that both two mutants reversed the insensitivity of *prt6* to ethylene and shortened the silique length as well (Figure 5B,C).

**Table 2.** Variant annotation in the candidate region of chromosome 5 with exonic variant function.

| Pos | Ref | Alt | Annotation | Annotation | SNP Index bulk1 | SNP Index bulk2 | deltaSNP | Short_Description |
|---|---|---|---|---|---|---|---|---|
| 4,251,301 | G | A | nonsynonymous | AT5G13280 | 0.33 | 0.88 | −0.55 | Aspartate kinase 1 |
| 4,469,182 | G | A | Stopgain | AT5G13840 | 0.43 | 0.87 | −0.43 | FIZZY-related 3 |
| 4,922,519 | G | A | nonsynonymous | AT5G15160 | 0.36 | 0.93 | −0.57 | BANQUO 2 |
| 5,070,109 | G | A | Stopgain | AT5G15580 | 0.34 | 0.88 | −0.53 | Longifolia1 (LNG1) |
| 5,361,835 | G | A | nonsynonymous | AT5G16390 | 0.42 | 0.94 | −0.52 | Chloroplastic acetylcoenzyme A carboxylase 1 |
| 6,113,584 | G | A | nonsynonymous | AT5G18440 | 0.36 | 0.91 | −0.55 | NULL |
| 6,133,091 | G | A | nonsynonymous | AT5G18480 | 0.41 | 0.89 | −0.48 | Plant glycogenin-like starch initiation protein 6 |
| 6,362,987 | G | A | nonsynonymous | AT5G19040 | 0.28 | 0.97 | −0.69 | Isopentenyltransferase 5 |
| 6,467,895 | G | A | nonsynonymous | AT5G19230 | 0.45 | 0.97 | −0.52 | Glycoprotein membrane precursor |
| 6,854,241 | G | A | nonsynonymous | AT5G20300 | 0.41 | 0.92 | −0.51 | Avirulence induced gene (AIG1) family protein |
| 7,354,380 | G | A | nonsynonymous | AT5G22190 | 0.35 | 0.94 | −0.58 | NULL |
| 7,610,318 | A | T | nonsynonymous | AT5G22794 | 0.99 | 0.99 | 0.00 | NULL |

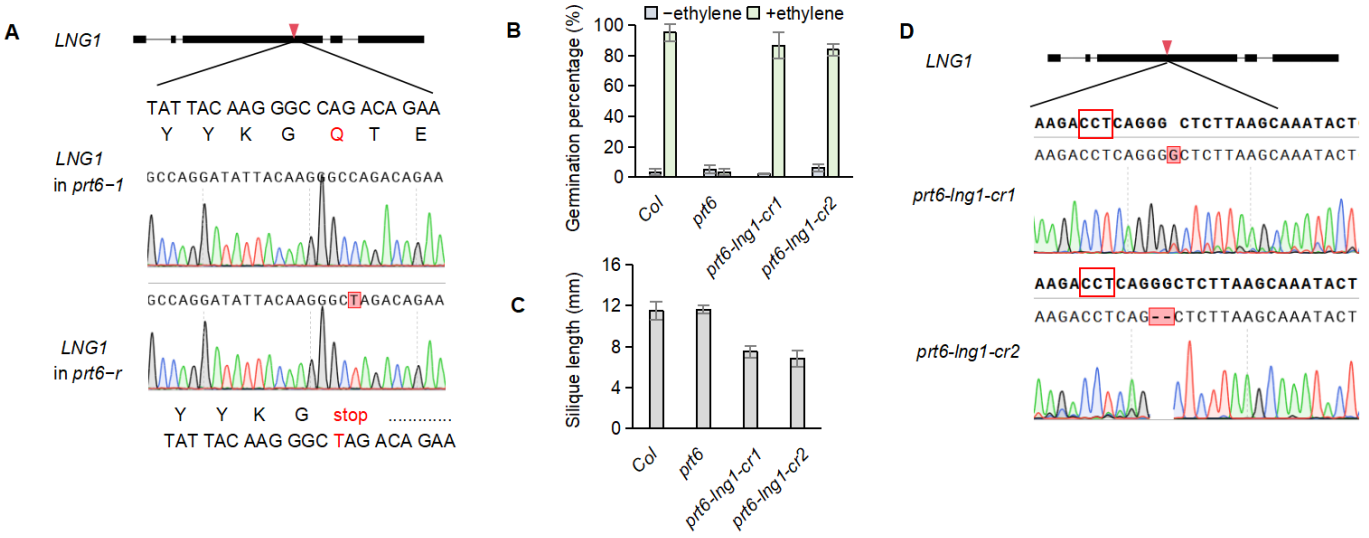


**Figure 5.** Gene function confirmation of *LNG1*. (**A**) Sequence analysis of *LNG1* in *prt6* and in *prt6−r* EMS mutant; (**B**) Seed germination with or without ethylene treatment at 25 °C in darkness; (**C**) Silique length measurement; *prt6-lng1-cr1* and *prt6-lng1-cr2* represent two mutants of *lng1* generated by Crispr-Cas9 technology in the background of *prt6−1*; (**D**) Sequence analysis of Crispr-Cas9 mediated gene editing of *LNG1*. The red arrow in Figure 5A,D represents the mutation site. The red solid square in Figure 5A,D represents mismatch in squence alignment. The red hallow squares in Figure 5D represents PAM sequence.

## 4. Discussion

Here, we identified a new allele, *LNG1*, that reversed the insensitivity of *prt6−1* to ethylene with the forward genetic method, suggesting that *LNG1* acted downstream of both ethylene signaling and the N-degron pathway to regulate seed dormancy. An EMS-mutagenized population was generated in the *prt6−1* background, and a stable mutant displaying enhanced germination under ethylene treatment and shortened siliques was isolated. These dual phenotypes enabled quantitative trait analysis. An F2 population derived from this mutant was subjected to BSA-seq, and both the G′ statistic and ΔSNP-index approaches identified a significant interval on chromosome 5. Variant annotation within this interval revealed a C-to-T transition in *LNG1* that introduces a premature stop codon.

CRISPR/Cas9-mediated complementation of *LNG1* fully restored ethylene sensitivity in *prt6−1*, confirming that the mutation in *LNG1* is responsible for the observed phenotypes.

The conventional QTL mapping requires phenotyping and genotyping of individuals from a large population, which is labor-intensive and time-consuming. BSA, an elegant method that has been used by genotyping DNA pools with extreme phenotypes, which overcome the disadvantage of QTL mapping [39,41]. BSAseq reduced the cost, simplified the analytical process without compromising the statistical power. For the purpose of being more efficient and fruitful, comparatively high sequencing depth and coverage are required to distinguish significant SNP-trait associations [39]. In our study, the sequencing data of the bulks were well-qualified with more than 99% coverage and more than 100× depth, which were prerequisites for a productive BSA-seq experiment (Table 1). The calculation and comparison of allele frequencies in the pools allow us to identify genomic regions with frequencies differing significantly between bulks. The key to the BSA approach was that the alleles of a locus controlling the trait would be enriched in either bulk, which was determined by the well-constructed two extreme bulks [41]. In our case, one parent, *prt6−1*, exhibited insensitivity to ethylene during seed germination and displayed normal silique length, whereas the other parent, *prt6−r*, showed heightened sensitivity to ethylene and shortened silique length. Though the quantitative traits we investigated here were easily affected, the recruitment of the two traits and the preliminary exclusion of low dormant seeds that germinated at 25 °C without ethylene improved the accuracy of the bulk construction.

Some software packages, such as QTL-seq and QTLseqr have been developed to carry out BSA-seq in the population of F2 populations, recombinant inbred lines (RILs), and backcross populations, whereas the software Mutmap (version 2.3.9) is especially for the F2 progeny from a cross between the original cultivar and the mutant [34,35,42]. In order to localize genomic positions of Arabidopsis genes controlling seed traits including the responsiveness to ethylene in germination and seed silique length, several BSA-seq analysis methods were employed. The G-statistic value for each SNP was calculated through the G-test using both REF and ALT SNPs in each bulk [39]. The higher G-statistic value represented by SNP nearby was linked with the trait. Whatever the G-statistic or ΔSNP index, a sliding window algorithm is integrated for visualization. The calculated statistics for each window were compared to a threshold to determine if the window contains a statistically significant association. Windows with values exceeding the threshold are considered to harbor a trait-associated region [35]. All the BSAseq methods in our study repeatedly localize the significant QTL on the chromosome 5, which confirmed the accuracy of the analysis (Figures 3 and 4, Supplementary Figure S2). In order not to miss any potential variants, the largest genomic region generated by QTLseq with the ΔSNP index was used for further variant annotation. The location of the final validated variant in the *LNG1* was also included in the significant regions produced by G' statistic method and the Mutmap method.

BSA-seq of the F2 generations of *prt6* × *prt6−r* identified that *LNG1* was epistatic to *PRT6*. Considering that LNG1 was not initiated with Met-Cys, we speculated that LNG1 was not able to be degraded by PRT6, at least in its form of pre-pro-protein, hinting that there might exist an unknown bridge between them, the mechanism of which awaited future exploration. It was previously reported that *LNG1* was known to regulate cell size in the longitudinal direction, the over-expression of which elongated the size of leaves, petals, and siliques [40]. While in the present study, we proposed that *LNG1* also participated in the regulation of seed germination under ethylene treatment. *LNG1*, as a multifunctional protein is implicated in both developmental patterning (cell elongation) and environmental adaptation (seed dormancy); its precise biochemical function remains a

key open question. It is clearly an important integrator of hormonal signals, particularly ethylene, and proteolytic regulation via the N-degron pathway. Future research should focus on (1) identifying the molecular partners and substrates of the LNG1 protein; (2) determining how its activity or expression is regulated by the N-degron pathway and ethylene; (3) investigating whether its role in cell elongation is also connected to hormonal signaling networks.

## 5. Conclusions and Perspectives

Our finding provides a new response to ethylene and a component epistatic to *PRT6* in seed germination control by forward genetic screening and reverse genetic verification. This result lays the foundation for future detailed molecular studies. In our study, we found that *PRT6-R* (*LNG1*) positively regulates both seed dormancy (at least in response to ethylene) and silique length in *Arabidopsis thaliana*. This raises the intriguing possibility that its homologues in other crops may exert similar pleiotropic effects. If this is confirmed, for example, in rapeseed, up-regulating the corresponding homolog via genome editing could simultaneously reduce pre-harvest sprouting and increase crop yield.

**Supplementary Materials:** The following supporting information can be downloaded at: https://www.mdpi.com/article/10.3390/seeds4040048/s1, Figure S1: The distribution of SNP-index values of bulk1 (A) and bulk2 (B) across all the five chromosomes generated by QTLseq; Figure S2: The distribution of SNP-index values across all the five chromosomes generated by Mutmap; Figure S3: Screening of positive T0 generation by glufosinate ammonium treatment; Figure S4: Relative expression of *LNG1* in knock-off plant seeds; Datasets S1, S2 and S3: Overview of the variants; Highly linked genomic regions by G' value method; Primers used in this study.

**Author Contributions:** Conceptualization, X.W. and Y.X.; methodology, X.W.; software, X.W.; validation, X.W.; formal analysis, X.W.; investigation, X.W., Y.L., Y.C. and Y.G.; resources, F.C.; data curation, X.W.; writing—original draft preparation, X.W.; writing—review and editing, X.W., Y.X. and F.C.; visualization, X.W.; supervision, Y.X.; project administration, Y.X.; funding acquisition, X.W. All authors have read and agreed to the published version of the manuscript.

**Funding:** This research was funded by GuangDong Basic and Applied Basic Research Foundation, grant number 2025A1515011011.

**Institutional Review Board Statement:** Not applicable.

**Informed Consent Statement:** Not applicable.

**Data Availability Statement:** The original contributions presented in this study are included in the article/Supplementary Material. Further inquiries can be directed to the corresponding author(s).

**Conflicts of Interest:** The authors declare no conflicts of interest.

## References

1. Finch-Savage, W.E.; Leubner-Metzger, G. Seed dormancy and the control of germination. *New Phytol.* **2006**, *171*, 501–523. [CrossRef]
2. Finch-Savage, W.E.; Footitt, S. Seed dormancy cycling and the regulation of dormancy mechanisms to time germination in variable field environments. *J. Exp. Bot.* **2017**, *68*, 843–856. [CrossRef]
3. Matilla, A.J.; Matilla-Vázquez, M.A. Involvement of ethylene in seed physiology. *Plant Sci.* **2008**, *175*, 87–97. [CrossRef]
4. Arc, E.; Sechet, J.; Corbineau, F.; Rajjou, L.; Marion-Poll, A. ABA crosstalk with ethylene and nitric oxide in seed dormancy and germination. *Front. Plant Sci.* **2013**, *4*, 63. [CrossRef]
5. Corbineau, F.; Xia, Q.; Bailly, C.; El-Maarouf-Bouteau, H. Ethylene, a key factor in the regulation of seed dormancy. *Front. Plant Sci.* **2013**, *5*, 539. [CrossRef] [PubMed]
6. Corbineau, F. Ethylene, a signaling compound involved in seed germination and dormancy. *Plants* **2024**, *13*, 2674. [CrossRef] [PubMed]

7. Kamaluddin, M.; Zwiazek, J.J. Ethylene enhances water transport in hypoxic Aspen. *Plant Physiol.* **2002**, *128*, 962–969. [CrossRef] [PubMed]
8. Arc, E.; Galland, M.; Godin, B.; Cueff, G.; Rajjou, L. Nitric oxide implication in the control of seed dormancy and germination. *Front. Plant Sci.* **2013**, *4*, 346. [CrossRef]
9. Prusinski, J.; Khan, A.A. Relationship of ethylene production to stress alleviation in seeds of lettuce cultivars. *J. Am. Soc. Hortic. Sci.* **1990**, *115*, 294–298. [CrossRef]
10. El-Maarouf-Bouteau, H.; Sajjad, Y.; Bazin, J.; Langlade, N.; Cristescu, S.M.; Balzergue, S.; Baudouin, E.; Bailly, C. Reactive oxygen species, abscisic acid and ethylene interact to regulate sunflower seed germination. *Plant Cell Environ.* **2015**, *38*, 364–374. [CrossRef]
11. Wang, K.L.C.; Li, H.; Ecker, J.R. Ethylene Biosynthesis and Signaling Networks. *Plant Cell* **2002**, *14*, S131. [CrossRef] [PubMed]
12. Merchante, C.; Alonso, J.M.; Stepanova, A.N. Ethylene signaling: Simple ligand, complex regulation. *Curr. Opin. Plant Biol.* **2013**, *16*, 554–560. [CrossRef] [PubMed]
13. Beaudoin, N.; Serizet, C.; Gosti, F.; Giraudat, J. Interactions between abscisic acid and ethylene signaling cascades. *Plant Cell* **2000**, *12*, 1103–1115. [CrossRef]
14. Siriwitayawan, G.; Geneve, R.L.; Downie, A. Seed germination of ethylene perception mutants of tomato and *Arabidopsis*. *Seed Sci. Res.* **2003**, *13*, 303–314. [CrossRef]
15. Chiwocha, S.D.; Cutler, A.J.; Abrams, S.R.; Ambrose, S.J.; Yang, J.; Ross, A.R.; Kermode, A.R. The *etr1−2* mutation in *Arabidopsis thaliana* affects the abscisic acid, auxin, cytokinin and gibberellin metabolic pathways during maintenance of seed dormancy, moist-chilling and germination. *Plant J.* **2005**, *42*, 35–48. [CrossRef]
16. Li, X.; Chen, T.; Li, Y.; Wang, Z.; Cao, H.; Chen, F.; Li, Y.; Soppe, W.J.J.; Li, W.; Liu, Y. *ETR1/RDO3* regulates seed dormancy by relieving the inhibitory effect of the ERF12-TPL complex on *DELAY OF GERMINATION1* expression. *Plant Cell* **2019**, *31*, 832–847. [CrossRef] [PubMed]
17. Jurdak, R.; Launay-Avon, A.; Paysant-Le Roux, C.; Bailly, C. Retrograde signalling from the mitochondria to the nucleus translates the positive effect of ethylene on dormancy breaking of *Arabidopsis thaliana* seeds. *New Phytol.* **2021**, *229*, 2192–2205. [CrossRef]
18. Graciet, E.; Wellmer, F. The plant N-end rule pathway: Structure and functions. *Trends Plant Sci.* **2010**, *15*, 447–453. [CrossRef]
19. Sriram, S.M.; Kim, B.Y.; Kwon, Y.T. The N-end rule pathway: Emerging functions and molecular principles of substrate recognition. *Nat. Rev. Mol. Cell Biol.* **2011**, *12*, 735–747. [CrossRef]
20. Gibbs, D.J.; Lee, S.C.; Isa, N.M.; Gramuglia, S.; Fukao, T.; Bassel, G.W.; Correia, C.S.; Corbineau, F.; Theodoulou, F.L.; Bailey-Serres, J.; et al. Homeostatic response to hypoxia is regulated by the N-end rule pathway in plants. *Nature* **2011**, *479*, 415–418. [CrossRef]
21. Licausi, F.; Kosmacz, M.; Weits, D.A.; Giuntoli, B.; Giorgi, F.M.; Voesenek, L.A.; Perata, P.; van Dongen, J.T. Oxygen sensing in plants is mediated by an N-end rule pathway for protein destabilization. *Nature* **2011**, *479*, 419–422. [CrossRef]
22. Gibbs, D.J.; Tedds, H.M.; Labandera, A.-M.; Bailey, M.; White, M.D.; Hartman, S.; Sprigg, C.; Mogg, S.L.; Osborne, R.; Dambire, C.; et al. Oxygen-dependent proteolysis regulates the stability of angiosperm polycomb repressive complex 2 subunit VERNALIZATION 2. *Nat. Commun.* **2018**, *9*, 5438. [CrossRef] [PubMed]
23. Weits, D.A.; Kunkowska, A.B.; Kamps, N.C.W.; Portz, K.M.S.; Packbier, N.K.; Nemec Venza, Z.; Gaillochet, C.; Lohmann, J.U.; Pedersen, O.; van Dongen, J.T.; et al. An apical hypoxic niche sets the pace of shoot meristem activity. *Nature* **2019**, *569*, 714–717. [CrossRef] [PubMed]
24. Labandera, A.-M.; Tedds, H.M.; Bailey, M.; Sprigg, C.; Etherington, R.D.; Akintewe, O.; Kalleechurn, G.; Holdsworth, M.J.; Gibbs, D.J. The PRT6 N-degron pathway restricts VERNALIZATION 2 to endogenous hypoxic niches to modulate plant development. *New Phytol.* **2021**, *229*, 126–139. [CrossRef]
25. Holman, T.J.; Jones, P.D.; Russell, L.; Medhurst, A.; Ubeda Tomas, S.; Talloji, P.; Marquez, J.; Schmuths, H.; Tung, S.A.; Taylor, I.; et al. The N-end rule pathway promotes seed germination and establishment through removal of ABA sensitivity in Arabidopsis. *Proc. Natl. Acad. Sci. USA* **2009**, *106*, 4549–4554. [CrossRef]
26. Gibbs, D.J.; Isa, N.M.; Movahedi, M.; Lozano-Juste, J.; Mendiondo, G.M.; Berckhan, S.; Marin-de la Rosa, N.; Conde, J.V.; Correia, C.S.; Pearce, S.P.; et al. Nitric oxide sensing in plants is mediated by proteolytic control of group VII ERF transcription factors. *Mol. Cell* **2014**, *53*, 369–379. [CrossRef]
27. Wang, X.; Gomes, M.M.; Bailly, C.; Nambara, E.; Corbineau, F. Role of ethylene and proteolytic N-degron pathway in the regulation of Arabidopsis seed dormancy. *J. Integr. Plant Biol.* **2021**, *63*, 2110–2122. [CrossRef]
28. Wang, X.; Yesbergenova-Cuny, Z.; Biniek, C.; Bailly, C.; El-Maarouf-Bouteau, H.; Corbineau, F. Revisiting the role of ethylene and N-end rule pathway on chilling-induced dormancy release in Arabidopsis seeds. *Int. J. Mol. Sci.* **2018**, *19*, 3577. [CrossRef] [PubMed]
29. Li, J.; Chory, J. Preparation of DNA from Arabidopsis. In *Arabidopsis Protocols*; Springer: Berlin/Heidelberg, Germany, 1998; pp. 55–60.
30. Chen, S. Ultrafast one-pass FASTQ data preprocessing, quality control, and deduplication using fastp. *iMeta* **2023**, *2*, e107. [CrossRef]

31. Li, H. Aligning sequence reads, clone sequences and assembly contigs with BWA-MEM. *arXiv* **2013**, arXiv:1303.3997. [CrossRef]
32. Li, H.; Handsaker, B.; Wysoker, A.; Fennell, T.; Ruan, J.; Homer, N.; Marth, G.; Abecasis, G.; Durbin, R.; Genome Project Data Processing Supgroup. The sequence alignment/map format and SAMtools. *Bioinformatics* **2009**, *25*, 2078–2079. [CrossRef]
33. McKenna, A.; Hanna, M.; Banks, E.; Sivachenko, A.; Cibulskis, K.; Kernytsky, A.; Garimella, K.; Altshuler, D.; Gabriel, S.; Daly, M.; et al. The Genome Analysis Toolkit: A MapReduce framework for analyzing next-generation DNA sequencing data. *Genome Res.* **2010**, *20*, 1297–1303. [CrossRef]
34. Sugihara, Y.; Young, L.; Yaegashi, H.; Natsume, S.; Shea, D.J.; Takagi, H.; Booker, H.; Innan, H.; Terauchi, R.; Abe, A. High-performance pipeline for MutMap and QTL-seq. *PeerJ* **2022**, *10*, e13170. [CrossRef] [PubMed]
35. Mansfeld, B.N.; Grumet, R. QTLseqr: An R Package for Bulk Segregant Analysis with Next-Generation Sequencing. *Plant Genome* **2018**, *11*, 180006. [CrossRef]
36. Wang, K.; Li, M.; Hakonarson, H. ANNOVAR: Functional annotation of genetic variants from high-throughput sequencing data. *Nucleic Acids Res.* **2010**, *38*, e164. [CrossRef] [PubMed]
37. Clough, S.J.; Bent, A.F. Floral dip: A simplified method for Agrobacterium-mediated transformation of *Arabidopsis thaliana*. *Plant J.* **1998**, *16*, 735–743. [CrossRef]
38. Greene, E.A.; Codomo, C.A.; Taylor, N.E.; Henikoff, J.G.; Till, B.J.; Reynolds, S.H.; Enns, L.C.; Burtner, C.; Johnson, J.E.; Odden, A.R.; et al. Spectrum of chemically induced mutations from a large-scale reverse-genetic screen in Arabidopsis. *Genetics* **2003**, *164*, 731–740. [CrossRef] [PubMed]
39. Magwene, P.M.; Willis, J.H.; Kelly, J.K. The statistics of bulk segregant analysis using next generation sequencing. *PLoS Comput. Biol.* **2011**, *7*, e1002255. [CrossRef]
40. Lee, Y.K.; Kim, G.T.; Kim, I.J.; Park, J.; Kwak, S.S.; Choi, G.; Chung, W.I. *LONGIFOLIA1* and *LONGIFOLIA2*, two homologous genes, regulate longitudinal cell elongation in Arabidopsis. *Development* **2006**, *133*, 4305–4314. [CrossRef]
41. Zou, C.; Wang, P.; Xu, Y. Bulked sample analysis in genetics, genomics and crop improvement. *Plant Biotechnol. J.* **2016**, *14*, 1941–1955. [CrossRef]
42. Takagi, H.; Abe, A.; Yoshida, K.; Kosugi, S.; Natsume, S.; Mitsuoka, C.; Uemura, A.; Utsushi, H.; Tamiru, M.; Takuno, S.; et al. QTL-seq: Rapid mapping of quantitative trait loci in rice by whole genome resequencing of DNA from two bulked populations. *Plant J.* **2013**, *74*, 174–183. [CrossRef] [PubMed]


**Disclaimer/Publisher's Note:** The statements, opinions and data contained in all publications are solely those of the individual author(s) and contributor(s) and not of MDPI and/or the editor(s). MDPI and/or the editor(s) disclaim responsibility for any injury to people or property resulting from any ideas, methods, instructions or products referred to in the content.